Organic LETTERS

Letter

pubs.acs.org/OrgLett

Filicinic Acid Based Meroterpenoids with Anti-Epstein–Barr Virus Activities from *Hypericum japonicum*

Linzhen Hu,[†,‡,∥] Yu Zhang,[‡,∥] Hucheng Zhu,[†] Junjun Liu,[†] Hua Li,[†] Xiao-Nian Li,[§] Weiguang Sun,[†] Junfen Zeng,[⊥] Yongbo Xue,[†] and Yonghui Zhang*[,†]

[†]School of Pharmacy, Tongji Medical College, Huazhong University of Science and Technology, Wuhan 430030, P. R. China

[‡]Union Hospital, Tongji Medical College, Huazhong University of Science and Technology, Wuhan 430022, P. R. China

[§]Kunming Institute of Botany, Chinese Academy of Sciences, Kunming 650204, P. R. China

[⊥]Department of Pharmacy, Renmin Hospital of Wuhan University, Wuhan 430060, P. R. China

Supporting Information

ABSTRACT: Seven filicinic acid–based meroterpenoids (**1**–**7**), possessing 6/6/11, 6/6/7/5, or 6/6/10 ring systems, were isolated from *Hypericum japonicum*. All of them have novel skeletons with the incorporation of sesquiterpenoid moieties to an acylated filicinic acid. Compounds **2a** and **4** exhibited significant efficacy on anti-Epstein–Barr virus, with EC_{50} values of 0.57 and 0.49 μM, respectively. Furthermore, compounds **2a** and **4** were well accommodated to the binding pocket of 2GV9 predicted by the molecular docking.

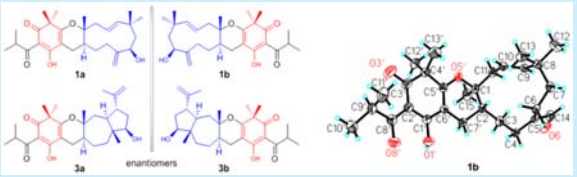

Hypericum (Guttiferae) has triggered abundant investigations by the scientific community[1] because of its phloroglucinol derivatives, which have diversiform structures and appealing pharmacological activities, e.g., antidepressant,[2] antibacterial,[3] anticancer,[4] and antiviral[5] properties. Our previous studies on *Hypericum* revealed metabolites with fascinating chemical structures and potential anti-HIV-1 characteristics.[6] Based on our exhaustive biochemical research on this genus, we focused on *H. japonicum* and obtained a series of bioactive compounds (**1**–**7**, Figure 1) with novel scaffolds, namely, hyperjaponols A–G, most of which presented remarkable anti-Epstein–Barr virus (EBV) activities.

As generalized by Singh et al., compounds **1**–**7** belong to the range of phloroglucinol–terpene adducts.[5] Numerous examples in the literature have been previously reported as diverse phloroglucinol–terpene adducts from *Eucalyptus*, *Psidium*, and *Kunzea* of the family Myrtaceae,[7] whose skeletons could be classified into three types (Figure S1): (I) involving chroman ring formation; (II) without chroman ring formation; and (III) involving spirocyclic formation. In this case, hyperjaponols A–G (**1**–**7**) (containing three pairs of enantiomers (**1a**/**1b**–**3a**/**3b**) and a pair of epimers (**5** and **6**)), as the phloroglucinol–sesquiterpene adducts of type **I**, possess novel skeletons with the incorporation of sesquiterpenoid moieties to an unexpected acylated filicinic acid via a hetero-Diels–Alder cycloaddition to form unusual 6/6/11, 6/6/7/5, or 6/6/10 ring systems. To the best of our knowledge, this is the first report about the filicinic acid based meroterpenoids possessing humulene, isodaucene, and germacrane/germacrene sesquiterpenoid motifs, which represent a new subclass of meroterpenoids. Herein, we described the isolation/enantioseparation, structure elucidation, bioactivity profiling, and a plausible biogenetic pathway toward these isolates. Preliminary molecular mechanisms of compounds **2a** and **4** toward anti-EBV activities were also explored using a small-scale inverse docking process and a microscale thermophoresis (MST) analysis.

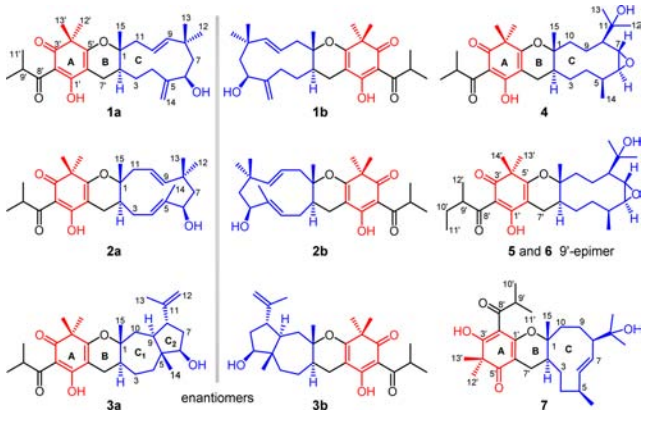

Figure 1. Structures of **1**–**7**.

(±)-Hyperjaponol A (**1a**/**1b**) has a molecular formula of $C_{28}H_{40}O_5$ as revealed by its HRESIMS data ($[M + H]^+$ m/z 457.2944; calcd for $C_{28}H_{41}O_5$, 457.2954). The enantiomeric property of **1a**/**1b** was tackled by an enantioseparation procedure (Figure 2). The ^{1}H NMR spectrum of **1** showed signals assignable to seven methyls [δ_H 1.01 (s), 1.07 (s), 1.09 (s), 1.12 (d, J = 6.8 Hz), 1.14 (d, J = 6.8 Hz), 1.28 (s), and 1.35 (s)], one olefinic methylene [δ_H 5.19 (s) and 4.93 (s)], an oxygenated methine [δ_H

Received: March 30, 2016
Published: April 26, 2016

DOI: 10.1021/acs.orglett.6b00906
Org. Lett. 2016, 18, 2272–2275

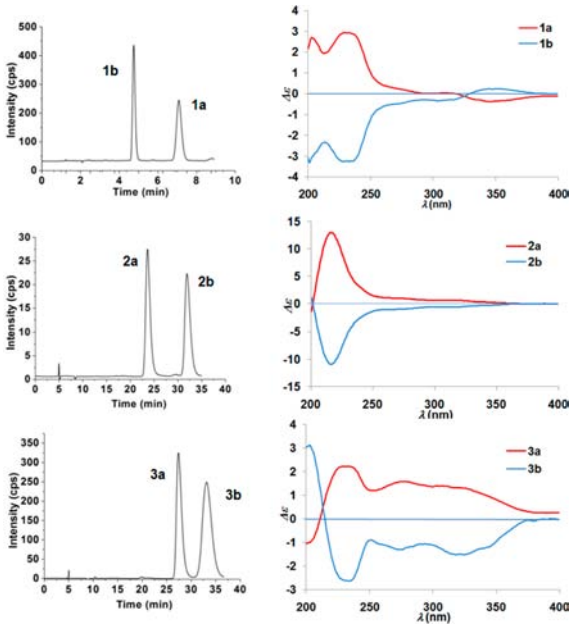

Figure 2. Enantioseparation chromatograms (left column) and experimental ECD spectra (right column) of enantiomers **1a**/**1b**–**3a**/**3b**.

3.87 (br d, J = 9.0 Hz)], and two olefinic methine protons [δ_H 5.14 (ddd, J = 15.8, 10.0, 4.0 Hz), and 5.36 (br d, J = 15.8 Hz)]. Its ^{13}C NMR displayed 28 carbon resonances resolved into 10 quaternary carbons (including two carbonyls and five olefinic carbons), five methines (including one oxygenated and two olefinic ones), six methylenes (including an olefinic one), and seven methyls. Considering that the indices of hydrogen deficiency are nine, compound **1** was speculated to have a tricyclic ring system.

The planar structure of **1** was elucidated on the basis of $^1H-^1H$ COSY and HMBC experiments (Figure 3). The spin systems of

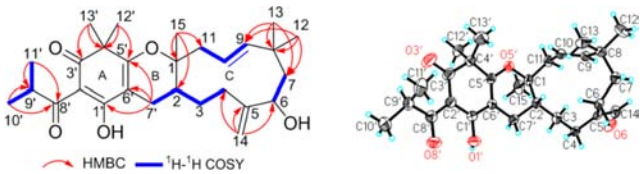

Figure 3. Key 2D correlations of **1** and X-ray structure of **1b**.

H-2/H-3/H-4, H-6/H-7, and H-9/H-10/H-11 in the $^1H-^1H$ COSY spectrum and HMBC correlations from Me-15 to C-1, C-2, and C-11, from H-14 to C-4, C-5, and C-6, and from Me-12 and Me-13 to C-7, C-8, and C-9 led to the construction of the macrocycle ring C, which appears to be an unusual humulene unit. In addition, HMBC correlations from Me-12′ and Me-13′ to C-3′, C-4′, and C-5′ and from H-7′ to C-1′, C-5′, and C-6′ together with the unassigned quaternary carbon at δ_C 104.8 suggested the existence of a methylated phloroglucinol motif (ring A), which was identified as a filicinic acid core by referring to sarothralin.[8] Combining the chemical shift of C-8′ (δ_C 208.0), the isobutyryl group revealed by HMBC correlations from Me-10′ and Me-11′ to C-8′ and C-9′ was preliminarily placed at C-2′. Finally, the linkage of rings A and C via C-7′ was indicted by the $^1H-^1H$ COSY cross-peak of H-7′/H-2, and ring B was created to satisfy the former mentioned degrees of unsaturation (Figure 3).

The relative stereochemistry of unit C was proposed by analyzing the NOESY interactions (Figure S2) and $^1H-^1H$ coupling constant. The large coupling constant of J between H-9 and H-10 (J = 15.8 Hz) suggested an E geometry of the double bond ($\Delta^{9,10}$). Subsequently, the NOESY correlations of H-10/H-2, H-10/H-6, and H-2/H-6 indicated that these protons were cofacial, and they were arbitrarily assigned as α-oriented. Furthermore, the observed NOESY cross-peaks of Me-15/H-11b and H-11b/H-9 together with the absence of relevant NOESY cross-peaks between H-2 and Me-15 suggested that Me-15 should be set as β orientation (Figure S2).

A single crystal of **1b** was successfully obtained, and X-ray crystallography analysis with Cu Kα radiation resulted in a Flack parameter of 0.11(8),[9] allowing an explicit assignment of absolute conformation as 1*S*,2*R*,6*S* (Figure 3; CCDC 1039176). Meanwhile, the absolute configuration of **1a** was assigned as 1*R*,2*S*,6*R* since **1a**/**1b** is a pair of enantiomers with identical NMR data and opposite ECD curves (Figure 2).

(±)-Hyperjaponol B (**2a**/**2b**) shared the same molecular formula of $C_{28}H_{40}O_5$ as **1** based on HRESIMS and ^{13}C NMR data. Detailed comparison of its NMR data with those of **1** indicated that the main differentiation between **2** and **1** was the absence of terminal double bond signals and the presence of an additional methyl (Me-14, δ_H 1.52; δ_C 11.0) and an olefinic methine (C-4, δ_H 5.12; δ_C 130.4) in **2**, which suggested that the terminal double bond in **1** was replaced by an endodouble bond in **2**. The structure and relative configuration of **2** were further confirmed by $^1H-^1H$ COSY, HMBC, and NOESY spectra (Figure S2), and the chiral stereochemistries of **2a** and **2b** were designated as 1*R*,2*S*,6*R* and 1*S*,2*R*,6*S* by the calculated ECD spectra (Figure 4).

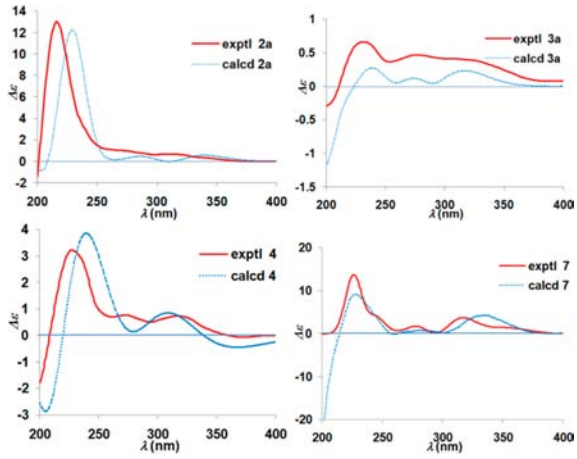

Figure 4. Experimental and calculated ECD spectra of **2a**, **3a**, **4**, and **7**.

(±)-Hyperjaponol C (**3a**/**3b**), which also consists of a pair of enantiomers, had the same molecular formula of $C_{28}H_{40}O_5$ as **1** and **2**. Comparison of the ^1H and ^{13}C NMR data (Tables S1 and S2) of **3** with those of **1** revealed that rings A and B in compound **3** were identical to those of **1**, while the sesquiterpenoid moiety was different. Analysis of the $^1H-^1H$ COSY spectrum of **3** yielded two spin systems viz. H-2/H-3/H-4 and H-6/H-7/H-8/H-9/H-10 (Figure S2). Furthermore, HMBC correlations from Me-14 to C-4, C-5, C-6, and C-9 and from Me-15 to C-1, C-2, and C-10 revealed a core structure with a sesquiterpenoid bicyclic ring system. In addition, HMBC correlations from Me-13 to C-8, C-11, and C-12 and from H-12 to C-8 and C-11 suggested the presence of an isopropenyl located at C-8. These interpretations

DOI: 10.1021/acs.orglett.6b00906
Org. Lett. 2016, 18, 2272–2275

allowed the assignment of the unit as an isodaucene skeleton (rings C_1 and C_2), a type of sesquiterpene rarely found in natural products.[10] The planar structure of **3**, possessing an unexpected 6/6/7/5 tetracyclic framework, was finally determined by detailed analyses of the ^{1}H−^{1}H COSY and HMBC spectra (Figure S2).

The stereochemistry of the isodaucene moiety of **3** was deduced by rigorous NOESY correlation analyses (Figure S2). NOESY interactions of H-2/H-4a, H-4a/H-6, H-6/H-7a, H-12a/Me-13, and Me-13/H-9 suggested that these protons were coaxial and were assigned the α-orientation. Simultaneously, NOESY signals of Me-14 with H-4b, H-10b, and H-8, together with H-8 with H-7b and H-12b, indicated that the mentioned protons should be defined to as β-oriented. Moreover, NOESY correlations of H-2/H-7′a and Me-15/H-7′b showed that Me-15 should be assigned as β orientation. Thus, the relative configuration of **3** was elucidated as shown in Figure S2. The absolute configuration of **3a** was determined as 1*R*,2*S*,5*R*,6*R*,8*R*,9*S* by the calculated ECD spectrum (Figure 4), which matched well with the result of $[Rh_2(OCOCF_3)_4]$ complex[11] of **3b** (Figure S3).

The overall patterns of the 1D NMR data (Tables S1 and S2) of hyperjaponol D (**4**) were very similar to those of **1**−**3**, except for the sesquiterpenoid part. Extensive analyses of its 2D NMR data suggested a germacrane sesquiterpenoid as follows: ^{1}H−^{1}H COSY cross-peaks of H-2−H-10 and HMBC correlations from Me-15 to C-1, C-2, and C-10 constructed the 10-membered ring C; HMBC correlations from Me-12 and Me-13 to C-8 and C-11 revealed the presence of a 2-hydroxyisopropyl at C-8; and the ^{1}H−^{1}H COSY cross-peak between Me-14 and H-5 confirmed the methyl group at C-5. An epoxy ring at C-6 (δ_C 61.1) and C-7 (δ_C 54.4) was proposed, according to their characteristic chemical shifts, to satisfy the degrees of unsaturation.

NOESY correlations of Me-15 with H-3b, H-3b with H-14, and H-14 with H-7 elucidated that these protons were coaxial and β-oriented (Figure S2). Meanwhile, NOESY cross-peaks of H-2 with H-8 and H-8 with H-6 implied that the mentioned protons were α-oriented (Figure S2). Finally, the consistency of the experimental and calculated ECD curves (Figure 4) unequivocally demonstrated that the chiral properties of **4** were 1*R*,2*S*,5*S*,6*S*,7*S*,8*R*.

Hyperjaponols E and F (**5** and **6**) were isolated as a pair of C-9′ epimers via chiral separation (Figure S4). The structures of **5** and **6** closely resembled that of **4**, with the only difference being that **5** and **6** possess an α-methylbutyryl group at C-2′ instead of the isobutyryl group in **4** (Figure 1), as revealed by their 1D and 2D NMR spectra. Unambiguous analyses of key 2D NMR correlations (Figure S2) and experimental ECD spectra (Figure S3) verified the relative and absolute configurations of the sesquiterpenoid moieties of **5** and **6**, which were identical with that of **4**. However, the relative configuration of C-9′ could not be determined in this case.

The sesquiterpenoid moiety of hyperjaponol G (**7**) was similar to those of **4**−**6** except that a double bond ($\Delta^{6,7}$) replaced the epoxy rings in the latter. The ^{13}C NMR data of ring A of **1**−**6** were exceedingly similar; however, the ^{13}C NMR data of **7** in the low field-shifted resonances were appreciably different from the aforementioned meroterpenoids (Table S2). The crucial NOESY correlations of H-9′/H-9 finally revealed that ring B of **7** was molded between C-1 and C-1′ via an oxygen atom rather than between C-1 and C-5′ as in **1**−**6** (Figure S2). Definitively, the experimental ECD band of **7** was in accordance with the calculated one (Figure 4), which confirmed the 1*R*,2*S*,5*S*,8*R*-stereogenic centers of **7**.

Hitherto, antipodes of compounds **4**−**7** have not been found in the present study. Hyperjaponols A−G (**1**−**7**) were initially discovered with 6/6/11, 6/6/7/5, or 6/6/10 ring systems from *H. japonicum*. All of them have novel skeletons with the incorporation of sesquiterpenoid moieties to an acylated filicinic acid. The putative biosynthetic route of compounds **1**−**7** was proposed as shown in Scheme S1 with the hetero-Diels−Alder cycloaddition as the key step.

The inhibitory activities of **1**−**7** on the lytic replication of EBV in B95-8 cells were assessed using a qPCR assay to measure the intracellular viral DNA copy numbers.[12] The results revealed that most of these substances exhibited prominent effects (Table 1 and Figure S5). In particular, compounds **2a** and **4** substantially inhibited EBV DNA replication with EC_{50} values of 0.57 and 0.49 μM and selectivity indexes of higher than 52.63 and of 106.78, respectively, approximately 5-fold more efficacy than a frequently used drug ganciclovir (EC_{50} 2.86 μM; selectivity index 104.50).

Table 1. Anti-EBV Activities of 1−7 (μM)

compd	CC_{50} [a]	EC_{50} [b]	selectivity index
1a	>41.35	10.33	>4.00
1b	>300	119.4	>2.50
2a	>30	0.57	>52.63
2b	>120	6.60	>18.18
3a	31.75		
3b	17.78		
4	48.05	0.49	106.78
5	60.49	17.53	3.45
6	41.62	14.47	2.87
7	>300	>300	
ganciclovir	>300	2.86	>104.50

[a] 50% cytotoxic concentration. [b] 50% effective concentration.

Since anti-herpes virus drugs such as ganciclovir, acyclovir, and penciclovir owe their inhibitory activities to targeting viral DNA polymerase,[12,13] eight enzymes (Table S3) involving DNA replication were selected to dock with compounds **1**−**7** with in silico target identification by performing a small-scale inverse docking,[14] and MST, a new technology to quantitatively measure the affinity between enzyme and compounds, was chosen to further confirm our hypothesis.[15] The calculated results of docking scores (Table S3) showed that 2GV9 (all DNA polymerase) had lower calculated binding energy, which implied that DNA polymerase might be the target on inhibition of EBV DNA replication by compounds **2a** and **4**. The MST results showed the well-matching binding affinities with the results of anti-EBV activities (Table S4). Furthermore, compounds **2a** and **4** were well accommodated to one of the binding pockets of DNA polymerase 2GV9 in a stretching conformation, which exhibited the ability to form key hydrophobic interactions with residues Phe470, Tyr557, Phe381, and Pro561, hydrogen bonds with Lys1069, and key electrostatic interaction with Asn466 (Figure 5).

In summary, hyperjaponols A−G (**1**−**7**), which possess hybrid structures of acylfilicinic acid moieties and diverse sesquiterpenoid motifs bearing unusual 6/6/11, 6/6/7/5, and 6/6/10 ring systems, were isolated from *H. japonicum*. We assessed, for the first time, the inhibitory effects of phloroglucinols on EBV genomic DNA replication, and (+)-hyperjaponols B (**2a**) and D (**4**) exhibited overwhelming potency comparing to a most

DOI: 10.1021/acs.orglett.6b00906
Org. Lett. 2016, 18, 2272−2275

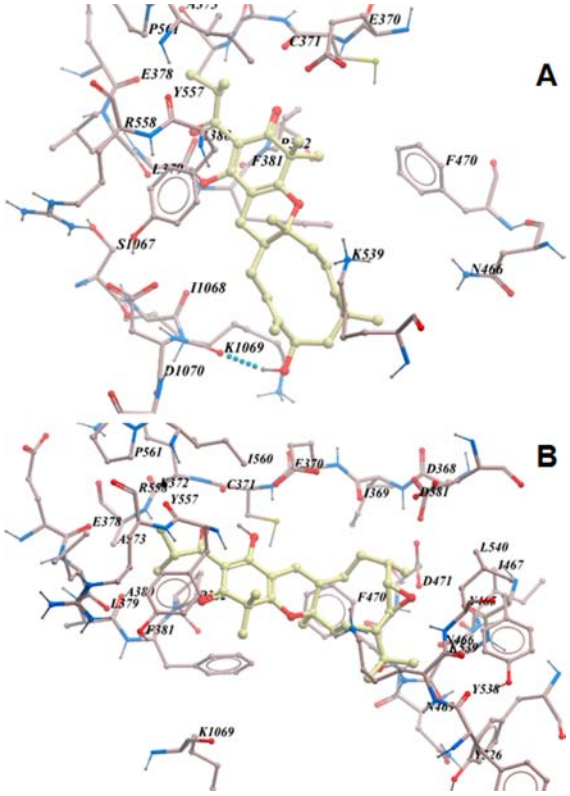

Figure 5. Binding poses of **2a** (A) and **4** (B) bound to 2GV9.

effective drug ganciclovir in vitro. Furthermore, compounds **2a** and **4** were well accommodated to the binding pocket of 2GV9 predicted by the molecular docking. Our future studies will focus on investigating feasible synthetic routes for **2a** and **4** or their analogues and gaining insight into the underlying molecular mechanisms of this unprecedented class of compounds.

■ ASSOCIATED CONTENT

Supporting Information

The Supporting Information is available free of charge on the ACS Publications website at DOI: 10.1021/acs.orglett.6b00906.

Experimental procedures, 1D and 2D NMR, MS, UV, and IR spectra for **1**−**7**, and detailed ECD calculations of **2a**, **3a**, **4**, and **7** (PDF)

X-ray crystallographic data of **1b** (CIF)

Generated docking model of compounds with 2GV9 (PDB)

Generated docking model of compounds with 2GV9 (PDB)

■ AUTHOR INFORMATION

Corresponding Author

*E-mail: zhangyh@mails.tjmu.edu.cn.

Author Contributions

‖L.H. and Y.Z. contributed equally.

Notes

The authors declare no competing financial interest.

■ ACKNOWLEDGMENTS

This work was financially supported by the Program for New Century Excellent Talents in University, the State Education Ministry of China (2008-0224), and the National Natural Science Foundation of China (Nos. 81573316, 31200258, 21502057, and 31500281).

■ REFERENCES

(1) (a) Grenning, A. J.; Boyce, J. H.; Porco, J. A., Jr. *J. Am. Chem. Soc.* **2014**, *136*, 11799−11804. (b) Singh, I. P.; Sidana, J.; Bharate, S. B.; Foley, W. J. *Nat. Prod. Rep.* **2010**, *27*, 393−416. (c) Richard, J. A.; Pouwer, R. H.; Chen, D. Y. K. *Angew. Chem., Int. Ed.* **2012**, *51*, 4536−4561. (d) Ciochina, R.; Grossman, R. B. *Chem. Rev.* **2006**, *106*, 3963−3986. (e) Gey, C.; Kyrylenko, S.; Hennig, L.; Nguyen, L. H. D; Buettner, A.; Pham, H. D.; Giannis, A. *Angew. Chem., Int. Ed.* **2007**, *46*, 5219−5222.

(2) Richard, J. A. *Eur. J. Org. Chem.* **2014**, *2014*, 273−299.

(3) Oya, A.; Tanaka, N.; Kusama, T.; Kim, S. Y.; Hayashi, S.; Kojoma, M.; Hishida, A.; Kawahara, N.; Sakai, K.; Gonoi, T.; Kobayashi, J. *J. Nat. Prod.* **2015**, *78*, 258−264.

(4) (a) Quiney, C.; Billard, C.; Salanoubat, C.; Fourneron, J. D.; Kolb, J. P. *Leukemia* **2006**, *20*, 1519−1525. (b) Zhang, S.; Yin, J.; Li, X.; Zhang, J.; Yue, R.; Diao, Y.; Li, H.; Wang, H.; Shan, L.; Zhang, W. *BMC Cancer* **2014**, *14*, 689−699.

(5) Singh, I. P.; Bharate, S. B. *Nat. Prod. Rep.* **2006**, *23*, 558−591.

(6) (a) Zhu, H.; Chen, C.; Yang, J.; Li, X. N.; Liu, J.; Sun, B.; Huang, S. X.; Li, D.; Yao, G.; Luo, Z.; Li, Y.; Zhang, J.; Xue, Y.; Zhang, Y. *Org. Lett.* **2014**, *16*, 6322−6325. (b) Li, D.; Xue, Y.; Zhu, H.; Li, Y.; Sun, B.; Liu, J.; Yao, G.; Zhang, J.; Du, G.; Zhang, Y. *RSC Adv.* **2015**, *5*, 5277−5287.

(7) (a) Bharate, S. B.; Khan, S. I.; Tekwani, B. L.; Jacob, M.; Khan, I. A.; Singh, I. P. *Bioorg. Med. Chem.* **2008**, *16*, 1328−1336. (b) Shao, M.; Wang, Y.; Jian, Y. Q.; Huang, X. J.; Zhang, D. M.; Tang, Q. F.; Jiang, W. X.; Sun, G.; Lv, Z. P.; Zhang, X. Q.; Ye, W. C. *Org. Lett.* **2012**, *14*, 5262−5265. (c) Yang, S. P.; Zhang, X. W.; Ai, J.; Gan, L. S.; Xu, J. B.; Wang, Y.; Su, Z. S.; Wang, L.; Ding, J.; Geng, M. Y.; Yue, J. M. *J. Med. Chem.* **2012**, *55*, 8183−8187. (d) Chenavas, S.; Fiorini Puybaret, C.; Joulia, P.; Larrouquet, C.; Waton, H.; Martinez, A.; Casabianca, H.; Fabre, B. *Phytochem. Lett.* **2015**, *11*, 69−73. (e) Shou, Q.; Smith, J. E.; Mon, H.; Brkljača, Z.; Smith, A. S.; Smith, D. M.; Griesser, H. J.; Wohlmuth, H. *RSC Adv.* **2014**, *4*, 13514−13517. (f) Shao, M.; Wang, Y.; Liu, Z.; Zhang, D. M.; Cao, H. H.; Fan, C. L.; Zhang, X. Q.; Chen, H. R.; Yao, X. S.; Ye, W. C. *Org. Lett.* **2010**, *12*, 5040−5043. (g) Tian, L. W.; Xu, M.; Li, X. C.; Yang, C. R.; Zhu, H. J.; Zhang, Y. J. *RSC Adv.* **2014**, *4*, 21373−21378. (h) Wu, L.; Luo, J.; Zhang, Y.; Zhu, M.; Wang, X.; Luo, J.; Yang, M.; Yu, B.; Yao, H.; Dai, Y.; Guo, Q.; Chen, Y.; Sun, H.; Kong, L. *Tetrahedron Lett.* **2015**, *56*, 229−232. (i) Wang, J.; Zhai, W. Z.; Zou, Y.; Zhu, J. J.; Xiong, J.; Zhao, Y.; Yang, G. X.; Fan, H.; Hamann, M. T.; Xia, G.; Hu, J. F. *Tetrahedron Lett.* **2012**, *53*, 2654−2658.

(8) Ishiguro, K.; Yamaki, M.; Takagi, S.; Yamagata, Y.; Tomita, K. *J. Chem. Soc., Chem. Commun.* **1985**, 26−27.

(9) Flack, H. D.; Bernardinelli, G. *Chirality* **2008**, *20*, 681−690.

(10) (a) Ma, J. H.; Zhao, F.; Wang, Y.; Liu, Y.; Gao, S. Y.; Ding, L. Q.; Chen, L. X.; Qiu, F. *Org. Biomol. Chem.* **2015**, *13*, 8349−8358. (b) Xia, W. J.; Li, D. R.; Shi, L.; Tu, Y. Q. *Tetrahedron: Asymmetry* **2001**, *17*, 168−169. (c) Tchuendem, M. H.; Mbah, J. A.; Tsopmo, A.; Ayafor, J. F.; Sterner, O.; Okunjic, C. C.; Iwu, M. M.; Schuster, B. M. *Phytochemistry* **1999**, *52*, 1095−1099.

(11) Frelek, J.; Szczepek, W. J. *Tetrahedron: Asymmetry* **1999**, *10*, 1507−1520.

(12) Ballout, M.; Germi, R.; Fafi Kremer, S.; Guimet, J.; Bargues, G.; Seigneurin, J. M.; Morand, P. *J. Virol. Methods* **2007**, *143*, 38−44.

(13) (a) Billaud, G.; Thouvenot, D.; Morfin, F. *Infect. Disord.: Drug Targets* **2009**, *9*, 117−125. (b) Lin, J. C. *Tzu Chi Med. J.* **2005**, *17*, 1−10.

(14) Gupta, S. D.; Bommaka, M. K.; Mazaira, G. I.; Galigniana, M. D.; Subrahmanyam, C. V. S; Gowrishankar, N. L.; Raghavendra, N. M. *Int. J. Biol. Macromol.* **2015**, *80*, 253−259.

(15) Lange, O.; Wolf, C.; Dietze, J.; Elsaesser, J.; Morbitzer, R.; Lahaye, T. *Nucleic Acids Res.* **2014**, *42*, 7436−7449.

■ NOTE ADDED AFTER ASAP PUBLICATION

On May 6, 2016, the figure of HRESIMS of compound **1a**/**1b** in the Supporting Information was corrected.

DOI: 10.1021/acs.orglett.6b00906
Org. Lett. 2016, 18, 2272−2275